

Precision cosmology and quantum effects in the very early universe

Anzhong Wang

Institute for Advanced Physics & Mathematics,
Zhejiang University of Technology, Hangzhou

&

Physics Department, Baylor University, Waco, Texas

The Interdisciplinary Center for Theoretical Study, USTC
Hefei, July 3, 2014

Table of Contents

- Planckian Physics and Precision Cosmology
- The Uniform Asymptotic Approximations
- Power Spectra and Spectral Indices
- High-Order Corrections
- Conclusions and Future Plan

Based on the works:

- T. Zhu, AW, G. Cleaver, K. Kirsten, and Q. Sheng, “*Inflationary cosmology with nonlinear dispersion relations*,” PRD89 (2014) 043507 [arXiv:1308.1104].
- T. Zhu, AW, G. Cleaver, K. Kirsten, and Q. Sheng, “*Constructing analytical solutions of linear perturbations of inflation with modified dispersion relations*,” arXiv:1308.1104.
- T. Zhu and AW, “*Gravitational quantum effects in the light of BICEP2 results*,” Phys. Rev. D, *in press*, (2014) [arXiv:1403.7696].
- T. Zhu, AW, G. Cleaver, K. Kirsten, and Q. Sheng, “*Quantum effects on power spectra and spectral indices with higher-order corrections*,” arXiv:1405.5301.

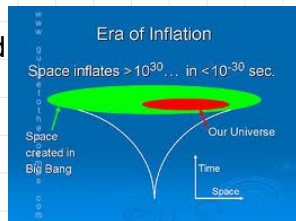
Table of Contents

- 1 Inflation and Planckian Physics**
- 2 The Uniform Asymptotic Approximations
- 3 Power Spectra and Spectral Indices
- 4 High-order Corrections
- 5 Conclusions and Future Plan

1.1 Why inflation?

(A. Guth, PRD23 (1981) 347)

- It solves most problems of standard big bang cosmology: **flatness, horizon, cosmic relics, etc.**
- It provides a causal mechanism for generations of **adiabatic, Gaussian, and nearly scale-invariant** primordial fluctuations, which leads to
 - the formation of large scale structure of the universe;
 - the Cosmic Microwave Background (CMB) anisotropies.
- Most predictions are matched to observations with high precision.¹

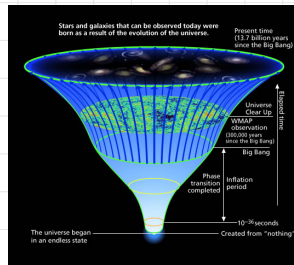


¹Planck Collaboration, arXiv:1303.5082; BICEP2 Collaboration, PRL112 (2014) 241101 [arXiv:1403.3985].

1.2 Trans-Planckian “Problem”

(Brandenberger and Martin, CGO30 (2013) 113001)

- During inflation, the wavelengths related to present observations, **were exponentially stretched**.
- The inflationary period is needed to be enough long to consistent with observations.



- If it is required to be more than 70 e-folds, the wavelengths corresponding to present observations, should be **smaller than the Planck length** at the beginning of the inflation—the **trans-Planckian “problem”**.

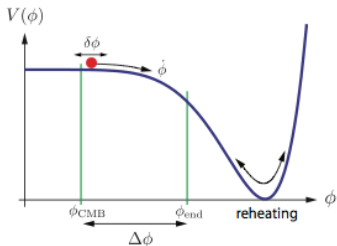
1.3 Planckian Excursion of Inflaton

(Lyth, PRL78 (1997) 1861)

- In the slow-roll approximations of a single scalar field, the change of the inflaton ϕ during inflation is given by,

$$\frac{\Delta\phi}{M_{\text{pl}}} \simeq \sqrt{\frac{r}{8}} \Delta N,$$

- M_{pl} : the Planck mass
- r : the ratio between the power spectra of tensor and scalar perturbations
- ΔN : the number of e-fold, corresponding to when the observed scales in the CMB leave the inflationary horizon



1.3 Planckian Excursion of Inflaton (Cont.)

- If r does not change as a function of N , this directly leads to

$$\frac{\Delta\phi}{M_{\text{pl}}} \simeq \mathcal{O}(1) \sqrt{\frac{r}{0.01}}.$$

- BICEP2 recently found for the first time that a non-zero value of the tensor-to-scalar ratio r at 7σ C.L., and estimated

$$r = 0.2^{+0.07}_{-0.05}.$$

- Obviously, $\Delta\phi$ exceeds the Planck scale if such a big r is confirmed.

1.3 Planckian Excursion of Inflaton (Cont.)

- As a result, the effective field theory (EFT) of inflation with a potential $V(\phi)$, which consists of power expansion of operators suppressed by Planck scale,

$$V(\phi) = V^{\text{eff}}(\phi) + \mathcal{O} \left[\left(\frac{\Delta\phi}{M_{\text{pl}}} \right)^n \right],$$

becomes questionable, and a theory with higher energy is demanded for a consistent treatment.

1.4 Extremely flat potential (the η - problem):

- Integrating out the UV physics at a scale M , it generically contributes to low-dimension operators in the EFT of the terms,

$$\delta\mathcal{L}_\phi = -\sqrt{-^{(4)}g} (c_0 M^4 + c_1 M^2 \phi^2),$$

c_0, c_1 : dimensionless constants of order 1.

- To have enough e-fold of the expansion, the potential of inflaton has to be extremely flat. This requires

$$\mu \ll H \simeq \frac{M^2}{M_{\text{pl}}}.$$

- However, it is very difficult to find such a scalar field, as it requires to control quantum interactions of gravitational strength. This is at present only possible in string theory.

1.5 Initial Conditions:

- Many inflationary scenarios only work if the fields are initially **very homogeneous and/or start with precise initial positions and velocities**. Any physical understanding of this requires a more complete formulation with ever-higher energies, such as string theory.

1.6 Quantum Fluctuations During Inflation

(D. Baumann, arXiv:0907.5424)

- According to the inflation paradigm, the large-scale structure of our universe and CMB all originated from **the quantum fluctuations produced during Inflation**. Such fluctuations can be mathematically classified as of **scalar, vector and tensor**.
- But, because of the expansion of the universe and particular nature of the fluctuations, vector perturbations did not grow, and observationally can be safely ignored.

1.6 Quantum Fluctuations During Inflation (Cont.)

- **Scalar** and **tensor** perturbations are described by mode functions $\mu_k(\eta)$,

$$\mu_k'' + \left(\omega_k^2 - \frac{z''}{z} \right) \mu_k = 0, \quad z \equiv \begin{cases} \frac{a\phi'}{\mathcal{H}}, & \text{scalar} \\ a, & \text{tensor} \end{cases} \quad (1)$$

- ω_k^2 : energy of the mode, given by,

$$\omega_k^2 = k^2, \quad (2)$$

in general relativity (GR)

- **k**: comoving wavenumber
- ϕ : the scalar field — the inflaton; and $\phi' \equiv d\phi/d\eta$
- η : the conform time, $d\eta \equiv dt/a(t)$
- $a(\eta)$: the expansion factor of the universe; and $\mathcal{H} \equiv a'/a$

1.6 Quantum Fluctuations During Inflation (Cont.)

- Power spectra, Δ_i^2 , are defined as,

$$\Delta_i^2 \equiv \frac{k^3}{2\pi^2} \left| \frac{\mu_k}{a} \right|_i^2, \quad (i = S, T).$$

- Then, the ratio r is given by

$$r \equiv \frac{\Delta_T^2}{\Delta_S^2} = \frac{8}{M_{pl}^2} \left(\frac{d\phi}{dN} \right)^2.$$

- Power induce are defined as

$$n_s \equiv 1 + \frac{d \ln \Delta_s^2(k)}{d \ln k}, \quad n_T \equiv \frac{d \ln \Delta_T^2(k)}{d \ln k}.$$

1.7 Quantum Effects on Inflation

- **String/M-Theory:** As the most promising candidate for a UV-completion of the Standard Model that unifies gauge and gravitational interaction in a consistent quantum theory, String/M theory can provide possibilities for an explicit realization of the inflationary scenario.
- String/M theory usually leads to a non-trivial time-dependent speed of sound for primordial perturbations ², for which the dispersion relation is modified to

$$\omega_k^2 = c_s^2(\eta)k^2, \quad (3)$$

- $c_s^2(\eta)$: the speed of sound, and could be very close to zero in the far UV regime.

²L. McAllister and E. Silverstein, *Gen. Rel. Grav.* 40, 565 (2007); C. P. Burgess, M. Cicoli, and F. Quevedo, arXiv: 1306.3512.

1.7 Quantum Effects on Inflation (Cont.)

- **Loop quantum cosmology (LQC):** Offers a natural framework to address the trans-Planckian issue and initial singularity, because effects of its underlying quantum geometry dominates at the Planck scale, leading to singularity resolution in a variety of cosmological models, where the initial singularity is replaced by the big bounce.
- Two kinds of quantum corrections to the cosmological background and perturbations: **holonomy and inverse-volume**³.

³M. Bojowald and G.M. Hossain, PRD78 (2008) 063547; M. Bojowald, G.M. Hossain, M. Kagan, and S. Shankaranarayanan, PRD79 (2009) 043505; 82, 109903 (E) (2010).

1.7 Quantum Effects on Inflation (Cont.)

- Due to the **holonomy** corrections, the dispersion relation in the mode functions is modified to

$$\omega_k^2 = \left(1 - 2\frac{\rho(\eta)}{\rho_c}\right) k^2 \quad (4)$$

- ρ_c : the energy density at which the big bounce happens.
- Due to the **inverse-volume** corrections, the dispersion relation in the mode functions is modified to

$$\omega_k^2 = k^2 \times \begin{cases} 1 + \left[\frac{\sigma\nu_0}{3} \left(\frac{\sigma}{6} + 1\right) + \frac{\alpha_0}{2} \left(5 - \frac{\sigma}{3}\right)\right] \delta_{\text{PL}}(\eta), & \text{scalar} \\ 1 + 2\alpha_0\delta_{\text{PL}}, & \text{tensor} \end{cases} \quad (5)$$

- α_0, ν_0, σ : encode the specific features of the model
- $\delta_{\text{PL}}(\eta)$: time-dependent, often given by $\delta_{\text{PL}} \sim a^{-\sigma}$.

1.7 Quantum Effects on Inflation (Cont.)

- To quantize gravity using quantum field theory, in 2009 Horava proposed a theory - Horava-Lifshitz (HL) gravity⁴, which is power-counting renormalizable, and has attracted lot of attention recently.
- In this theory, the dispersion relation is modified to [AW and R. Maartens, PRD81 (2010) 024009; AW, PRD82 (2010) 124063],

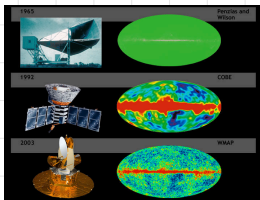
$$\omega_k^2(\eta) = k^2 - b_1 \frac{k^4}{a^2 M_*^2} + b_2 \frac{k^6}{a^4 M_*^4} \quad (6)$$

- M_* : the energy scale of the HL gravity
- b_1, b_2 : depend on the coupling constants of the HL theory and the type of perturbations, scalar or tensor.

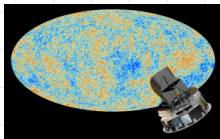
⁴P. Horava, PRD79 (2009) 084008.

1.8 Precision Cosmology

- Since the first measurement of CMB in 1964 by **Penzias and Wilson (PW)**, there have been a variety of experiments to measure its radiation anisotropies and polarization, such as **WMAP, PLAnck and BICEP2**, with ever increasing precision.



PW, COBE, WMAP



Planck



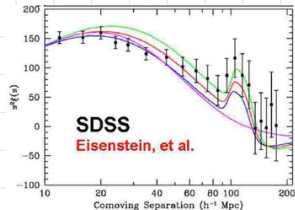
BICEP2

1.8 Precision Cosmology (cont.)

- In the coming decade, we anticipate that various new surveys will make even more **accurate (percentage level)** CMB measurements:
 - **Balloon experiments:** Balloon-borne Radiometers for Sky Polarisation Observations (BaR-SPOrT); The E and B Experiment (EBEX); ...
 - **Ground experiments:** Cosmology Large Angular Scale Surveyor (CLASS); Millimeter-Wave Bolometric Interferometer (MBI-B); Qubic; ...
 - **Space experiments:** Sky Polarization Observatory (SPOrT); ...

1.8 Precision Cosmology (cont.)

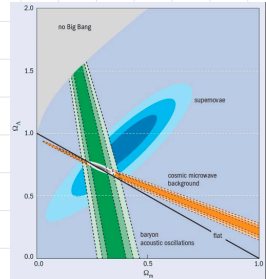
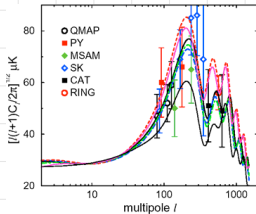
- In addition to CMB measurements, **Large-scale structure surveys, measuring the galaxy power spectrum and the position of the baryon acoustic peak**, have provided independently valuable information on the evolution of the universe.
- The first measurement of the kind started with the baryon acoustic oscillation (BAO) in the SDSS LRG and 2dF Galaxy surveys⁵.



⁵D.J. Eisenstein, et al., ApJ 633 (2005) 560; S. Cole, et al., MNRAS362 (2005) 505.

1.8 Precision Cosmology (cont.)

- Since then, various large-scale structure surveys have been carried out ⁶, and provided sharp constraint on the budgets that made of the universe.



⁶Tegmark, M., et al. 2006, Phys. Rev. D, 74, 123507; Percival, W. J., Nichol, R. C., Eisenstein, D. J., et al. 2007, ApJ, 657, 51; Kazin, E. A., et al. 2010, ApJ, 710, 1444; Blake, C., Kazin, E., Beutler, F., et al. 2011, MNRAS, 418, 1707.

1.8 Precision Cosmology (cont.)

- Various new surveys will make even more accurate measurements of the galaxy power spectrum:
 - Ground-Based: [the Prime Focus Spectrograph](#), [Big BOSS](#),
 - Space-based, [Euclid](#), [WFIRST](#),

1.8 Precision Cosmology (cont.)

- Therefore, predicting the precise power spectra of scalar and tensor perturbations and their spectral indices becomes an essential step in the interpretation of the data and in understanding the nature of the universe, including that of dark matter and dark energy.
- Cosmology indeed enters its **golden age** — the era of the **precision cosmology!**

Table of Contents

- 1 Inflation and Planckian Physics
- 2 The Uniform Asymptotic Approximations**
- 3 Power Spectra and Spectral Indices
- 4 High-order Corrections
- 5 Conclusions and Future Plan

2.1 Modified Equation of Mode Function

- Taking the quantum effects into account, either from [string/M-Theory](#), [loop Quantum Cosmology](#), or [HL gravity](#), mentioned above, the equation of motion for μ_k can be always cast in the form,

$$\frac{d^2 \mu_k(y)}{dy^2} = [g(y) + q(y)] \mu_k(y), \quad (7)$$

$g(y)$, $q(y)$: functions of $y [\equiv -k\eta]$, to be defined below.

- For example, in the HL gravity, we have

$$\begin{aligned} g(y) + q(y) &\equiv \left(\frac{z''}{z} - \omega_k^2 \right) k^{-2} \\ &= \frac{\nu^2 - 1/4}{y^2} - 1 + b_1 \epsilon_*^2 y^2 - b_2 \epsilon_*^4 y^4, \end{aligned} \quad (8)$$

with $\epsilon_* \equiv H/M_*$, $z''/z \equiv (\nu^2(\eta) - 1/4)/\eta^2$.

2.1 Modified Equation of μ_k (Cont.)

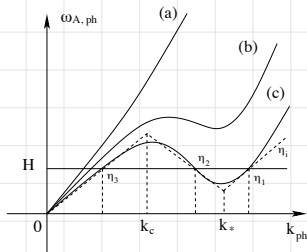
- It is remarkable to note that the evolution of the mode function with the non-linear dispersion relation given by Eq. (8) had been already studied since 2001⁷, **as toy models to mimic quantum effects.**
- This is well before 2009 when Horava first proposed his theory, in which this non-linear dispersion relation is **naturally produced as the result of power-counting renormalizability of the theory.**

⁷J. Martin and R.H. Brandenberger, PRD63 (2001) 123501; D65 (2002) 103514; D68 (2003) 063513; J.C. Niemeyer and R. Parentani, D64 (2001) 101301 (R); L. Bergstorm and U.H. Danielsson, JHEP12 (2002) 038; J. Martin and C. Ringeval, PRD69 (2004) 083515; R. Easther, W. H. Kinney, and H. Peiris, JCAP 05 (2005) 009; M.G. Jackson and K. Schalm, PRL 108 (2012) 111301.

2.1 Modified Equation of μ_k (Cont.)

- However, in all these studies, the Brandenberger-Martin (BM) approximation [PRD65 (2002) 103514] was used,

$$\mu_k(\eta) = \begin{cases} \frac{1}{\sqrt{2\omega_k(\eta)}} e^{-i \int_{\eta_i}^{\eta} \omega_k(\eta') d\eta'}, & \text{when } \eta < \eta_1, \\ C_+ a(\eta) + C_- a(\eta) \int_{\eta_1}^{\eta} \frac{d\eta'}{a^2(\eta')}, & \text{when } \eta_1 < \eta < \eta_2, \\ \frac{\alpha_k e^{-i \int_{\eta_2}^{\eta} \omega_k(\eta') d\eta'} + \beta_k e^{i \int_{\eta_2}^{\eta} \omega_k(\eta') d\eta'}}{\sqrt{2\omega_k(\eta)}}, & \text{when } \eta_2 < \eta < \eta_3, \\ D_+ a(\eta) + D_- a(\eta) \int_{\eta_3}^{\eta} \frac{d\eta'}{a^2(\eta')}, & \text{when } \eta > \eta_3. \end{cases}$$

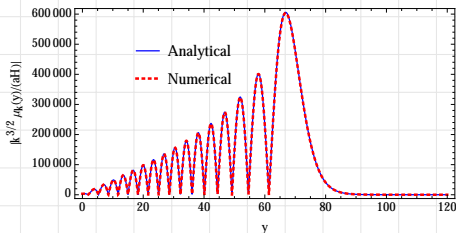


2.1 Modified Equation of μ_k (Cont.)

- Its validity in various physics situations has been questioned recently [S.E. Joras and G. Marozzi, PRD79 (2009) 023514]:
 - The approximations break down at the matching points (η_1 , η_2 , and η_3), and thus the errors becomes large.
 - Numerical calculations showed it is only valid when the comoving wavenumber $k \gg aH$.
 - The error bounds for the solutions are not known.

2.1 Modified Equation of μ_k (Cont.)

- In the following, I am going to present *the uniform approximation method*, developed recently by us, which has the following advantages:
 - The error bounds are given explicitly. By properly controlling them, the (analytical) solutions with high accuracy can be obtained, even only up to the first-order approximations.



(μ_k to the first-order approximation)

2.1 Modified Equation of μ_k (Cont.)

- Our method can be easily generalized to high-order approximations. In fact, recently we have obtained analytical solutions of the mode functions up to the third-order, where the error bounds are within 0.15%.
- Our method is applicable not only to the non-linear dispersion relation given by Eq.(8), but to any one that can be cast in the form (7).

2.1 Modified Equation of μ_k (Cont.)

- It should be noted that the uniform approximation method was first applied to study analytically the evolution of the mode function by Habib et al⁸, but they only studied the relativistic case

$$\omega_k^2 = k^2,$$

and up to the first-order approximations, for which the upper bounds of the errors are only $\lesssim 15\%$.

⁸S. Habib, K. Heitmann, G. Jungman, and C. Molina-Paris, PRL89 (2002) 281301; S. Habib, A. Heinen, K. Heitmann, G. Jungman, and C. Molina-Paris, PRD70 (2004) 083507 (2004); S. Habib, A. Heinen, K. Heitmann, and G. Jungman, PRD71 (2005) 043518.

2.1 Modified Equation of μ_k (Cont.)

- As to be shown below, it is not trivial at all to generalize it to the case with,
 - an arbitrary form of ω_k^2 ,

$$\frac{d^2 \mu_k(y)}{dy^2} = k^{-2} \left(\frac{z''(y)}{z(y)} - \omega_k^2(y) \right) \mu_k(y) \quad (9)$$

- high-order approximations, so the up bounds of the errors are $\lesssim 0.15\%$.

2.2 Liouville Transformations

- The strategy is to use the well-established Liouville transformations to introduce
 - a new function U , instead of μ_k ,
 - a new variable ξ , instead of y ,

$$\mu_k(y) \rightarrow U(\xi),$$

- so that the resulted equation can be solved
 - analytically order by order in terms of $\epsilon \equiv 1/\lambda \ll 1$, where

$$g(y) = \lambda^2 \hat{g}(y), \quad \left| \frac{\hat{g}(y)}{q(y)} \right| \simeq \mathcal{O}(1).$$

- the corresponding error bounds are well under control at each step, so the errors can be minimized.

2.2 Liouville Transformations (Cont.)

- The Liouville Transformations are

$$\begin{aligned}U(\xi) &= \chi^{1/4} \mu_k(y), & \chi &\equiv \xi'^2 = \frac{|g(y)|}{f^{(1)}(\xi)^2}, \\f(\xi) &= \int^y \sqrt{|g(y)|} dy, & f^{(1)}(\xi) &= \frac{df(\xi)}{d\xi},\end{aligned}\quad (10)$$

- χ must be regular and not vanish in the intervals of interest;
- $f^{(1)}(\xi)^2$ must be chosen so that it has zeros and singularities of the same type as that of $g(y)$.

2.2 Liouville Transformations (Cont.)

- The equation of motion for the mode function reduces to,

$$\frac{d^2 U(\xi)}{d\xi^2} = \left[\pm f^{(1)}(\xi)^2 + \psi(\xi) \right] U(\xi), \quad (11)$$

with

$$\psi(\xi) = \frac{q(y)}{\chi} - \chi^{-3/4} \frac{d^2(\chi^{-1/4})}{dy^2}, \quad (12)$$

in the above “+” for $g(y) > 0$, and “-” for $g(y) < 0$.

- Neglecting $\psi(\xi)$ we obtain solutions to the first-order approximation
- Choosing properly $f^{(1)}(\xi)^2$ in order for the equation to be solved analytically, and meanwhile minimizing the error bounds

2.2 Liouville Transformations (Cont.)

- To solve the differential equation for the new function $U(\xi)$ analytically, we divide the task into three steps:
 - Solve it near some singular points of $g(y) + q(y)$, often called **poles**, which are the points where $y = 0, \infty$ for

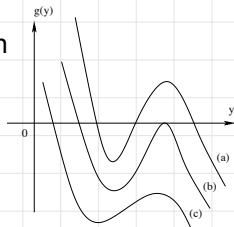
$$g(y) + q(y) = \frac{\nu^2 - 1/4}{y^2} - 1 + b_1 \epsilon_*^2 y^2 - b_2 \epsilon_*^4 y^4 \quad (13)$$

- Solve it near the **turning points**, or roots of the equation,

$$g(y) = 0. \quad (14)$$

For the case decrified by Eq.(13), it in general has three real roots, y_0, y_1 and y_2 .

- Then, matching all the solutions together to get a global one.



2.3 Solutions near poles

- To illustrate our method, in the following we shall restrict ourselves to the case,

$$g(y) + q(y) = \frac{\nu^2 - 1/4}{y^2} - 1 + b_1 \epsilon_*^2 y^2 - b_2 \epsilon_*^4 y^4 \quad (15)$$

although our method can be used for any function of $g(y) + q(y)$ or ω_k^2 .

2.3 Solutions near poles (Cont.)

- The functions $g(y)$ and $q(y)$ are well-defined near the two possible poles, 0^+ , $+\infty$. Thus, we choose

$$f^{(1)}(\xi)^2 = 1, \quad \xi = \int^y \sqrt{|g(y)|} dy, \quad (16)$$

so that

$$\frac{d^2 U(\xi)}{d\xi^2} = \left[\pm 1 + \psi(\xi) \right] U(\xi), \quad (17)$$

here “+” for 0^+ , and “-” for $+\infty$.

- By neglecting $\psi(\xi)$ as the first-order approximations, the solutions of the above equation can be determined analytically.

2.3 Solutions near poles (Cont.)

Near the pole 0^+ , the solutions are given by

$$\begin{aligned}\mu_k^+(y) = & \frac{c_+}{g(y)^{1/4}} e^{\int^y \sqrt{g(y)} dy} (1 + \epsilon_1^+) \\ & + \frac{d_+}{g(y)^{1/4}} e^{-\int^y \sqrt{g(y)} dy} (1 + \epsilon_2^+),\end{aligned}\quad (18)$$

$\epsilon_1^+, \epsilon_2^+$: represent the errors of the approximations,

$$\epsilon_1^+ = \frac{1}{2} \int_0^\xi \left(1 - e^{2(v-\xi)}\right) \psi(v) (1 + \epsilon_1^+) dv, \quad (19)$$

$\xi \in (0, a_1)$, $v \in (0, \xi]$, $y \in (0^+, \hat{a}_1)$;
 a_1, \hat{a}_1 : the upper bounds of the variables ξ, y
 $\xi(0^+) = 0$, $\xi(\hat{a}_1) = a_1$.

2.3 Solutions near poles (Cont.)

Similar expression is for ϵ_2^+ . Then, the error bounds are

$$\begin{aligned} |\epsilon_1^+|, \quad \frac{|d\epsilon_1^+/dy|}{2|g|^{1/2}} &\leq \exp\left(\frac{1}{2}\mathcal{V}_{0,y}(F)\right) - 1, \\ |\epsilon_2^+|, \quad \frac{|d\epsilon_2^+/dy|}{2|g|^{1/2}} &\leq \exp\left(\frac{1}{2}\mathcal{V}_{y,\hat{a}_1}(F)\right) - 1, \end{aligned} \quad (20)$$

where the error control function $F(y)$ and $\mathcal{V}_{a,b}(F)$ are defined as

$$\begin{aligned} F(y) &= \int \left[\frac{1}{|g|^{1/4}} \frac{d^2}{dy^2} \left(\frac{1}{|g|^{1/4}} \right) - \frac{q}{|g|^{1/2}} \right] dy, \\ \mathcal{V}_{a,b}(F) &\equiv \int_a^b \left| \frac{dF(y)}{dy} \right| dy \end{aligned} \quad (21)$$

2.3 Solutions near poles (Cont.)

Near the pole $+\infty$, the solutions are given by

$$\begin{aligned}\mu_k^-(y) = & \frac{c_-}{|g(y)|^{1/4}} e^{\int^y \sqrt{|g(y)|} dy} (1 + \epsilon_1^-) \\ & + \frac{d_-}{|g(y)|^{1/4}} e^{-\int^y \sqrt{|g(y)|} dy} (1 + \epsilon_2^-),\end{aligned}\quad (22)$$

ϵ_1^- , ϵ_2^- : represent the errors of the approximations, and have similar expressions as those for ϵ_1^+ , ϵ_2^+ .

2.4 Solutions near turning points

- Error Control Function and Choice of $g(y)$ and $q(y)$:

The convergence of the error control function $F(y)$ requires that one must choose [PRD89 (2014) 043507],

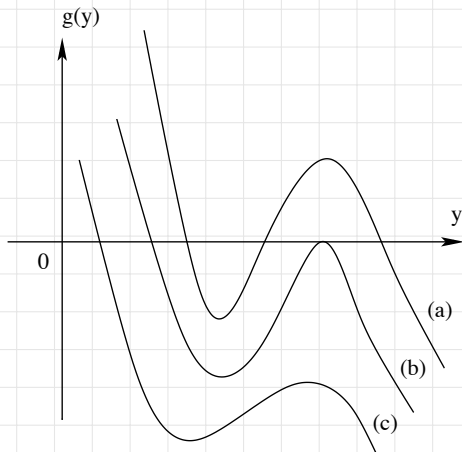
$$\begin{aligned}g(y) &= \frac{\nu^2}{y^2} - 1 + b_1 \epsilon_*^2 y^2 - b_2 \epsilon_*^4 y^4, \\q(y) &= -\frac{1}{4y^2}.\end{aligned}\tag{23}$$

- Then, $g(y)$, usually has three roots, (y_0, y_1, y_2) ,
 - we assume $0 < y_0 < \operatorname{Re}(y_1) \leq \operatorname{Re}(y_2)$
 - y_0 is always real and positive
 - when y_1, y_2 real, we assume $y_1 \leq y_2$
 - When y_1, y_2 are complex, we have $y_1 = y_2^*$.

2.4 Solutions near turning points (Cont.)

The turning points, defined as the roots of

$$g(y) = \frac{\nu^2}{y^2} - 1 + b_1 \epsilon_*^2 y^2 - b_2 \epsilon_*^4 y^4 = 0. \quad (24)$$



2.4 Solutions near turning points (Cont.)

- **Approximate solution around y_0 :** Since y_0 is a single zero of $g(y) = 0$, we can choose $f^{(1)}(\xi)^2 = \pm\xi$, so that

$$\frac{d^2U(\xi)}{d\xi^2} = \left(\xi + \psi(\xi)\right)U(\xi), \quad (25)$$

which has the approximate solution,

$$\begin{aligned} \mu_k(y) = & \alpha_0 \left(\frac{\xi}{g(y)}\right)^{1/4} \left(\text{Ai}(\xi) + \epsilon_3\right) \\ & + \beta_0 \left(\frac{\xi}{g(y)}\right)^{1/4} \left(\text{Bi}(\xi) + \epsilon_4\right), \end{aligned} \quad (26)$$

$\text{Ai}(\xi)$, $\text{Bi}(\xi)$: the Airy functions

ϵ_3 , ϵ_4 : the errors of the approximations

2.4 Solutions near turning points (Cont.)

- The error ϵ_3 is given by

$$\epsilon_3(\xi) = \int_{\xi}^{a_3} \mathcal{K}(\xi, v) |v|^{-1/2} \psi(v) \left(\mathbf{Ai}(v) + \epsilon_3 \right), \quad (27)$$

a_3 : the upper bound of ξ ; \hat{a}_3 : the upper bound of y , with $\xi(\hat{a}_3) = a_3$.

- A similar expression for ϵ_4 . Then, the up bounds are

$$\begin{aligned} \frac{|\epsilon_3|}{M(\xi)}, \quad \frac{|\partial \epsilon_3 / \partial \xi|}{N(\xi)} &\leq \frac{E^{-1}(\xi)}{\lambda} \left\{ \exp \left(\lambda \mathcal{V}_{\xi, a_3}(H) \right) - 1 \right\}, \\ \frac{|\epsilon_4|}{M(\xi)}, \quad \frac{|\partial \epsilon_4 / \partial \xi|}{N(\xi)} &\leq \frac{E(\xi)}{\lambda} \left\{ \exp \left(\lambda \mathcal{V}_{a_4, \xi}(H) \right) - 1 \right\}, \end{aligned} \quad (28)$$

but now with the error control function $H(y)$ defined as $H(\xi) = \int_{\xi}^{a_3} |v|^{-1/2} \psi(v) dv$.

2.4 Solutions near turning points (Cont.)

- Approximate solutions around $y = (y_1, y_2)$: Near these turning points, we choose

$$f^{(1)}(\xi)^2 = |\xi^2 - \xi_0^2|, \quad \xi_0^2 = \pm \frac{2}{\pi} \left| \int_{y_1}^{y_2} \sqrt{|g(y)|} dy \right|, \quad (29)$$

- ‘ ‘ \pm ’ ’ correspond $y_{1,2}$ are real and complex, respectively
- when $y_{1,2}$ are both real, ξ_0 is positive
- when $y_{1,2}$ are both complex, ξ_0 is purely imaginary
- when $y_1 = y_2$, they degenerate to a double turning point, and $\xi_0 = 0$

2.4 Solutions near turning points (Cont.)

- Then, the solutions around y_1 and y_2 are given by

$$\begin{aligned} \mu_k(y) = & \alpha_1 \left(\frac{\xi^2 - \xi_0^2}{-g(y)} \right)^{1/4} \left[W \left(\frac{1}{2} \xi^2, \sqrt{2} \xi \right) + \epsilon_5 \right] \\ & + \beta_1 \left(\frac{\xi^2 - \xi_0^2}{-g(y)} \right)^{1/4} \left[W \left(\frac{1}{2} \xi^2, -\sqrt{2} \xi \right) + \epsilon_6 \right], \end{aligned} \quad (30)$$

ϵ_5, ϵ_6 : the errors of the approximations

$W \left(\frac{1}{2} \xi^2, \pm \sqrt{2} \xi \right)$: the cylindrical functions

2.4 Solutions near turning points (Cont.)

- The error ϵ_5 is given by

$$\begin{aligned}\epsilon_5(\xi) &= \int_{\xi}^{a_5} \mathcal{K}(\xi, v) \frac{\psi(v)}{v} \left\{ \mathbb{W} \left(\frac{1}{2} \xi_0^2, \sqrt{2}v \right) + \epsilon_5 \right\} dv, \\ \mathcal{K}(\xi, v) &= v \left\{ \mathbb{W} \left(\frac{1}{2} \xi_0^2, \sqrt{2}\xi \right) \mathbb{W} \left(\frac{1}{2} \xi_0^2, -\sqrt{2}v \right) \right. \\ &\quad \left. - \mathbb{W} \left(\frac{1}{2} \xi_0^2, \sqrt{2}v \right) \mathbb{W} \left(\frac{1}{2} \xi_0^2, -\sqrt{2}\xi \right) \right\}. \quad (31)\end{aligned}$$

a_5 : is the upper bound of ξ .

- A similar expression is for ϵ_6 .

2.4 Solutions near turning points (Cont.)

- The up error bounds are

$$\begin{aligned} & \frac{|\epsilon_5|}{M\left(\frac{1}{2}\xi_0^2, \sqrt{2}\xi\right)}, \quad \frac{|\partial\epsilon_5/\partial\xi|}{\sqrt{2}N\left(\frac{1}{2}\xi_0^2, \sqrt{2}\xi\right)} \\ & \leq \frac{\kappa}{\lambda E\left(\frac{1}{2}\xi_0^2, \sqrt{2}\xi\right)} \left\{ \exp\left(\lambda\mathcal{Y}_{\xi, a_5}(\text{H})\right) - 1 \right\}, \quad (32) \end{aligned}$$

$$\begin{aligned} & \frac{|\epsilon_6|}{M\left(\frac{1}{2}\xi_0^2, \sqrt{2}\xi\right)}, \quad \frac{|\partial\epsilon_6/\partial\xi|}{\sqrt{2}N\left(\frac{1}{2}\xi_0^2, \sqrt{2}\xi\right)} \\ & \leq \frac{\kappa E\left(\frac{1}{2}\xi_0^2, \sqrt{2}\xi\right)}{\lambda} \left\{ \exp\left(\lambda\mathcal{Y}_{0, \xi}(\text{I})\right) - 1 \right\}. \quad (33) \end{aligned}$$

2.5 Matching to the Initial solution

- We assume the universe was initially at the adiabatic (Bunch-Davies) vacuum,

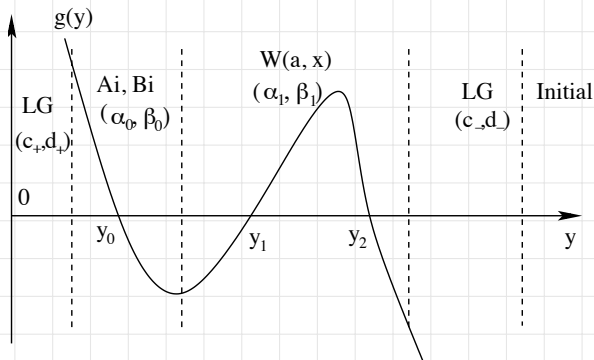
$$\begin{aligned}\lim_{y \rightarrow +\infty} \mu_k(y) &= \frac{1}{\sqrt{2\omega}} e^{-i \int \omega d\eta} \\ &\simeq \sqrt{\frac{k}{2}} \frac{1}{(-g)^{1/4}} \exp\left(-i \int_{y_i}^y \sqrt{-g} dy\right). \quad (34)\end{aligned}$$

- Since the equation of the mode function is second-order, we need one more condition to completely fix the free parameters in the solutions. We choose the second one as the Wronskian condition

$$\mu_k(y)\mu_k^*(y)' - \mu_k^*(y)\mu_k(y)' = i. \quad (35)$$

2.5 Matching to the Initial solution (Cont.)

- We found four sets of solutions:
 - LG solution near the pole $y = \infty$ with (c_-, d_-)
 - Cylindrical function solution near the two turning points $y_{1,2}$ with (α_1, β_1)
 - Airy function solution near the turning point y_0 with (α_0, β_0)
 - LG solution near the pole $y = 0$ with (c_+, d_+)



2.5 Matching to the Initial solution (Cont.)

- Using the initial conditions to the LG solution near the pole $y = \infty$, we find that

$$C_- = 0, \quad d_- = \sqrt{\frac{1}{2k}}. \quad (36)$$

- Matching the LG solution with the cylindrical function solutions at $y \gg y_2$ we find that

$$\begin{aligned} \alpha_1 &= 2^{-3/4} k^{-1/2} j^{-1/2}(\xi_0), \\ \beta_1 &= -i 2^{-3/4} k^{-1/2} j^{1/2}(\xi_0), \end{aligned} \quad (37)$$

with $j(\xi_0) \equiv \sqrt{1 + e^{\pi\xi_0^2}} - e^{\pi\xi_0^2/2}$.

2.5 Matching to the Initial solution (Cont.)

- Matching the cylindrical function solution with the Airy function one in their common region $y \in (y_0, y_1)$, we find

$$\begin{aligned}\alpha_0 &= \sqrt{\frac{\pi}{2k}} [j^{-1}(\xi_0) \sin \mathfrak{B} - ij(\xi_0) \cos \mathfrak{B}], \\ \beta_0 &= \sqrt{\frac{\pi}{2k}} [j^{-1}(\xi_0) \cos \mathfrak{B} + ij(\xi_0) \sin \mathfrak{B}],\end{aligned}\quad (38)$$

where

$$\begin{aligned}\mathfrak{B} &\equiv \int_{y_0}^{y_1} \sqrt{-g} dy + \phi(\xi_0^2/2), \\ \phi(x) &\equiv \frac{x}{2} - \frac{x}{4} \ln x^2 + \frac{1}{2} \text{ph}\Gamma\left(\frac{1}{2} + ix\right).\end{aligned}\quad (39)$$

2.5 Matching to the Initial solution (Cont.)

- Finally, matching the LG solution near the pole $y = 0$ with the Airy function one in their common region $y \in (0, y_0)$, we find

$$\begin{aligned}d_+ &= \frac{\alpha_0}{2\sqrt{\pi}} \exp\left(-\int_{0^+}^{y_0} \sqrt{g} dy\right), \\c_+ &= \frac{\beta_0}{\sqrt{\pi}} \exp\left(\int_{0^+}^{y_0} \sqrt{g} dy\right).\end{aligned}\tag{40}$$

2.6 Comparing with numerical (exact) solutions

- When $y_{1,2}$ are real and $y_1 \neq y_2$:

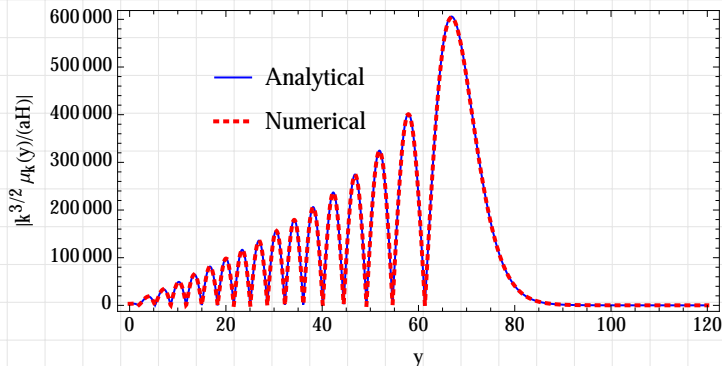


Figure : The numerical (exact) (red dotted curves) and analytical (blue solid curves) solutions with $b_1 = 3$, $b_2 = 2$, $\nu = 3/2$, and $\epsilon_* = 0.01$.

2.6 Comparing with numerical (exact) solutions (Cont.)

- When $y_{1,2}$ are real and $y_1 = y_2$:

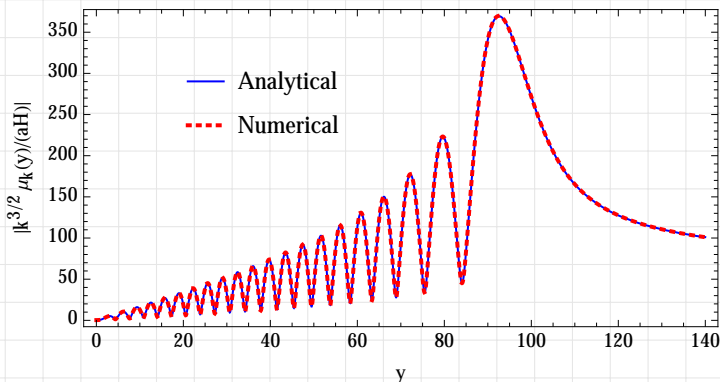


Figure : The numerical (exact) (red dotted curves) and analytical (blue solid curves) solutions with $b_1 = 2$, $b_2 = 1.00023$, $\nu = 3/2$, and $\epsilon_* = 0.01$.

2.6 Comparing with numerical (exact) solutions (Cont.)

- When $y_{1,2}$ are complex:

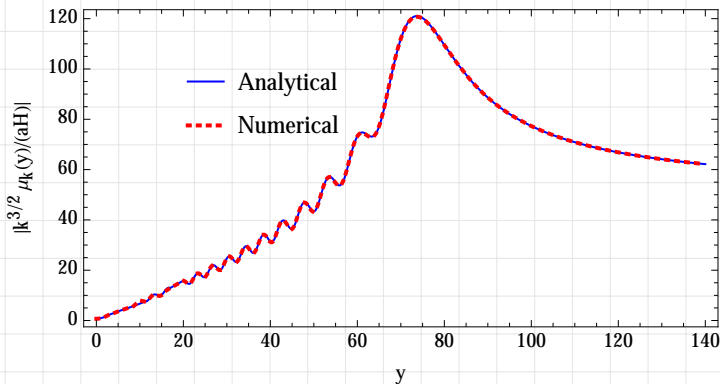


Figure : The numerical (exact) (red dotted curves) and analytical (blue solid curves) solutions with $b_1 = 3.5$, $b_2 = 3.2$, $\nu = 3/2$, and $\epsilon_* = 0.01$.

Table of Contents

- 1 Inflation and Planckian Physics
- 2 The Uniform Asymptotic Approximations
- 3 Power Spectra and Spectral Indices**
- 4 High-order Corrections
- 5 Conclusions and Future Plan

3.1 Power spectra

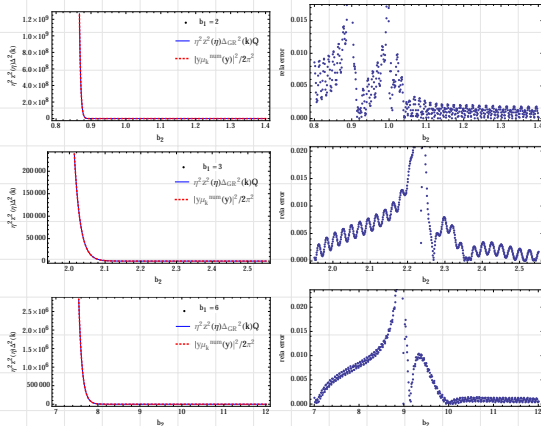
The power spectra (of scale or tensor modes) are calculated when $y \rightarrow 0^+$, thus one can only consider the growing mode of the solution. Then, we find,

$$\begin{aligned}\Delta^2(k) &= \frac{k^3}{2\pi^2} \left| \frac{\mu_k(y)}{z(\eta)} \right|^2 \\ &= \frac{k^3}{2\pi^3} \left(\frac{\beta_0^2}{z^2 \sqrt{g(y)}} \right) e^{2 \int_{y_0}^y \sqrt{g(y)} dy} \\ &\simeq \Delta_{\text{GR}}^2(k) \mathcal{Q},\end{aligned}\tag{41}$$

$$\mathcal{Q} = \frac{2k|\beta_0|^2}{\pi} \left(1 + \frac{5}{6} b_1 \nu^3 \epsilon_*^2 + \mathcal{O}(\epsilon_*^4) \right).\tag{42}$$

3.1 Power spectra (Cont.)

- Our analytical approximate results vs numerical (exact) ones: The error bounds in general are $\lesssim 15\%$.



3.2 Spectral indices

The scale and tensor spectral indices are given by

$$\begin{aligned}n_s &= 1 + \frac{d \ln \Delta_s^2(k)}{d \ln k} = 4 - 2\nu_s = n_s^{\text{GR}}, \\n_T &= \frac{d \ln \Delta_T^2(k)}{d \ln k} = 3 - 2\nu_T = n_T^{\text{GR}}\end{aligned}\quad (43)$$

- the scale and tensor spectral indices are the same as those in GR to the first order slow-roll approximation
- the modification factor \mathcal{Q} does not depend on k , thus does not have contributions to n_s and n_T .

Table of Contents

- 1 Inflation and Planckian Physics
- 2 The Uniform Asymptotic Approximations
- 3 Power Spectra and Spectral Indices
- 4 High-order Corrections**
- 5 Conclusions and Future Plan

4.1 Mode function $U(\xi)$

- For the sake of simplicity, in the following we consider the case where $g(y) = 0$ has only one real root, y_0 .
- The other cases in principle can be treated similarly, but the calculations are much more involved mathematically.
- Then, we can choose

$$f^{(1)}(\xi) = \pm \xi, \quad (44)$$

$\xi = \xi(y)$: a monotone decreasing function

“+”: corresponds to $g(y) \geq 0$

“-”: corresponds to $g(y) \leq 0$.

4.1 Mode function $U(\xi)$ (Cont.)

- Then, the mode function $U(\xi)$ is given by

$$\begin{aligned} U(\xi) = & \alpha_0 \left[\text{Ai}(\lambda^{2/3}\xi) \sum_{s=0}^n \frac{A_s(\xi)}{\lambda^{2s}} \right. \\ & \left. + \frac{\text{Ai}'(\lambda^{2/3}\xi)}{\lambda^{4/3}} \sum_{s=0}^{n-1} \frac{B_s(\xi)}{\lambda^{2s}} + \epsilon_3^{(2n+1)} \right] \\ & + \beta_0 \left[\text{Bi}(\lambda^{2/3}\xi) \sum_{s=0}^n \frac{A_s(\xi)}{\lambda^{2s}} \right. \\ & \left. + \frac{\text{Bi}'(\lambda^{2/3}\xi)}{\lambda^{4/3}} \sum_{s=0}^{n-1} \frac{B_s(\xi)}{\lambda^{2s}} + \epsilon_4^{(2n+1)} \right], \end{aligned} \tag{45}$$

where α_0 and β_0 are two integration constants.

4.1 Mode function $U(\xi)$ (Cont.)

- The coefficients A_s and B_s are given by

$$A_0(\xi) = 1,$$
$$B_s = \frac{\pm 1}{2(\pm\xi)^{1/2}} \int_0^\xi \{\psi(v)A_s(v) - A_s''(v)\} \frac{dv}{(\pm v)^{1/2}},$$
$$A_{s+1}(\xi) = -\frac{1}{2}B_s'(\xi) + \frac{1}{2} \int \psi(v)B_s(v)dv, (s = 0, 1, 2, \dots) \quad (46)$$

where “+” corresponds to $\xi \geq 0$, and “-” to $\xi \leq 0$.

4.1 Mode function $U(\xi)$ (Cont.)

- The errors $\epsilon_3^{(2n+1)}$ and $\epsilon_4^{(2n+1)}$ are given by,

$$\begin{aligned} & \frac{\epsilon_3^{(2n+1)}}{M(\lambda^{2/3}\xi)}, \quad \frac{\partial \epsilon_3^{(2n+1)}/\partial \xi}{\lambda^{2/3}N(\lambda^{2/3}\xi)} \\ & \leq 2E^{-1}(\lambda^{2/3}\xi) \exp \left[\frac{2\kappa_0 \mathcal{V}_{\alpha,\xi}(|\xi^{1/2}|B_0)}{\lambda} \right] \\ & \quad \times \frac{\mathcal{V}_{\alpha,\xi}(|\xi^{1/2}|B_n)}{\lambda^{2n+1}}, \\ & \frac{\epsilon_4^{(2n+1)}}{M(\lambda^{2/3}\xi)}, \quad \frac{\partial \epsilon_4^{(2n+1)}/\partial \xi}{\lambda^{2/3}N(\lambda^{2/3}\xi)} \\ & \leq 2E(\lambda^{2/3}\xi) \exp \left[\frac{2\kappa_0 \mathcal{V}_{\xi,\beta}(|\xi^{1/2}|B_0)}{\lambda} \right] \\ & \quad \times \frac{\mathcal{V}_{\xi,\beta}(|\xi^{1/2}|B_n)}{\lambda^{2n+1}}. \end{aligned} \tag{47}$$

4.1 Mode function $U(\xi)$ (Cont.)

- To determine α_0 and β_0 , we assume the same initial conditions as in the first-order approximations, that is, **the universe initially was in the Bunch-Davies vacuum, and μ_k satisfies the Wronskian condition,**

$$\lim_{y \rightarrow +\infty} \mu_k(y) = \frac{1}{\sqrt{2\omega_k}} e^{-i \int \omega_k d\eta}, \quad (48)$$

$$\mu_k(y) \mu_k^*(y)' - \mu_k^*(y) \mu_k(y)' = i. \quad (49)$$

- After tedious calculations, we surprisingly find a very simple result,

$$\alpha_0 = \sqrt{\frac{\pi}{2k}}, \quad \beta_0 = i \sqrt{\frac{\pi}{2k}}. \quad (50)$$

4.2 High-order Power spectra and spectral index

- To the third-order approximations, the power spectrum is given by

$$\begin{aligned}\Delta^2(k) &\equiv \frac{k^3}{2\pi^2} \left| \frac{\mu_k(y)}{z} \right|_{y \rightarrow 0^+}^2 \\ &= \frac{k^2}{4\pi^2} \frac{-k\eta}{z^2(\eta)\nu^2(\eta)} \exp\left(2 \int_y^{\nu_0} \sqrt{\hat{g}(\hat{y})} d\hat{y}\right) \\ &\quad \times \left[1 + \frac{H(+\infty)}{\lambda} + \frac{H^2(+\infty)}{2\lambda^2} + \mathcal{O}(1/\lambda^3) \right].\end{aligned}\tag{51}$$

4.2 High-order Power spectra and spectral index (Cont.)

- To the third-order approximations, the spectral index is given by

$$\begin{aligned}n - 1 &\equiv \frac{d \ln \Delta^2(k)}{d \ln k} \\ &\simeq 3 + 2 \int_y^{\nu_0} \frac{d\hat{y}}{\sqrt{\hat{g}(\hat{y})}} + \frac{1}{\lambda} \frac{dH(+\infty)}{d \ln k} \\ &\quad + \mathcal{O}\left(\frac{1}{\lambda^3}\right).\end{aligned}\tag{52}$$

4.3 Applications to General Relativity

- High-order power spectra and spectral indices have been calculated so far **only up to the second-order**, one in GR ($\omega_k^2 = k^2$)⁹, and the other in k-inflation ($\omega_k^2 = c_s^2(\eta)k^2$)¹⁰.
- **As a consistency check, we apply our general formulas developed above to GR, and then compare our results with the ones obtained above.**

⁹J.-O. Gong and E.D. Stewart, PLB510 (2001) 1; S.M. Leach, A, Liddle, J. Martin and D. Schwarz, PRD66 (2002) 023515; J.-O. Gong, CQG21 (2004) 5555; R. Casadio, et al, PRD71 (2005) 043517; PLB625 (2005) 1.

¹⁰J. Martin, C. Ringeval and V. Vennin, JCAP06 (2013) 021.

4.3 Applications to General Relativity (Cont.)

- To the second-order approximations, the scalar power spectrum is given by

$$\begin{aligned} \Delta_s^2(k) \simeq & \frac{181H_*^2}{72e^3\pi^2\epsilon_*} \left\{ 1 + \delta_{*1} \left(\ln 9 - \frac{134}{181} \right) + \epsilon_* \left(\ln 81 - \frac{630}{181} \right) \right. \\ & + \left(\frac{\pi^2}{3} - \frac{4195}{1629} + 4 \ln^2 3 - \frac{536 \ln 3}{181} \right) \epsilon_*^2 \\ & + \delta_{*1} \epsilon_* \left(\frac{5\pi^2}{12} - \frac{3944}{1629} + 3 \ln^2 3 - \frac{40 \ln 3}{181} \right) \\ & + \delta_{*1}^2 \left(-\frac{\pi^2}{12} + \frac{2146}{1629} + 3 \ln^2 3 - \frac{402 \ln 3}{181} \right) \\ & \left. + \delta_{*2} \left(\frac{\pi^2}{12} - \frac{172}{1629} - \ln^2 3 + \frac{134 \ln 3}{181} \right) \right\}. \end{aligned} \quad (53)$$

4.3 Applications to General Relativity (Cont.)

- Comparing it with the one obtained by the Green Function Method:

Methods	Amplitude	ϵ	δ_1	ϵ^2	$\delta_1\epsilon$	δ_1^2	δ_2
Uniform Approximation	$\frac{181H^2}{72e^3\pi^2\epsilon_*}$	0.913786	1.456893	2.28912	5.06928	1.67574	0.323269
Green function method	$\frac{H^2}{8\pi^2\epsilon_*}$	0.918549	1.459274	2.158558	4.907929	1.709446	0.290097
Relative difference	$\sim 0.13\%$	0.52%	0.16%	5.7%	3.2%	2.0%	10.3%

4.3 Applications to General Relativity (Cont.)

- To the second-order approximations, the scalar power spectral index is given by

$$\begin{aligned}n_s - 1 \simeq & -2\delta_{*1} - 4\epsilon_* + \epsilon_*^2 \left(8 \ln 3 - \frac{100}{9} \right) + \delta_{*1}\epsilon_* \left(10 \ln 3 - \frac{89}{9} \right) + \delta_{*1}^2 \left(\frac{7}{9} - \ln 9 \right) + \delta_{*2} \left(\ln 9 - \frac{7}{9} \right) \\ & + \epsilon_*^3 \left(\frac{4\pi^2}{3} - \frac{3488}{81} - 16 \ln^2 3 + \frac{472 \ln 3}{9} - \frac{8 \ln 64}{81} \right) + \delta_{*3} \left(\frac{\pi^2}{12} + \frac{17}{162} - \ln^2 3 + \frac{7 \ln 3}{9} - \frac{\ln 2}{27} \right) \\ & + \delta_{*1}\epsilon_*^2 \left(\frac{31\pi^2}{12} - \frac{8773}{162} - 31 \ln^2 3 + \frac{757 \ln 3}{9} - \frac{31 \ln 64}{162} \right) \\ & + \delta_{*1}^2\epsilon_* \left(\frac{\pi^2}{4} - \frac{91}{54} - 3 \ln^2 3 + \frac{19 \ln 3}{3} - \frac{\ln 2}{9} \right) + \delta_{*2}\epsilon_* \left(\frac{7\pi^2}{12} - \frac{757}{162} - 7 \ln^2 3 + \frac{121 \ln 3}{9} - \frac{7 \ln 2}{27} \right) \\ & + \delta_{*1}^3 \left(\frac{\pi^2}{6} - \frac{133}{81} - 2 \ln^2 3 + \frac{14 \ln 3}{9} - \frac{2 \ln 2}{27} \right) + \delta_{*1}\delta_{*2} \left(-\frac{\pi^2}{4} + \frac{83}{54} + 3 \ln^2 3 - \frac{7 \ln 3}{3} + \frac{\ln 2}{9} \right).\end{aligned}$$

4.3 Applications to General Relativity (Cont.)

- Comparing it with the one obtained by the Green Function Method:

TABLE II: Compare the uniform approximation and Green function method

Methods	ϵ	δ_1	ϵ^2	$\delta_1\epsilon$	δ_1^2	δ_2
Uniform Approximation	-2	-4	-2.32221	1.09723	-1.41945	1.41945
Green function method	-2	-4	-2.162903	1.296372	-1.459274	1.459274
Relative difference	0%	0%	6.8%	15%	2.7%	2.7%

4.3 Applications to General Relativity (Cont.)

- To the second-order approximations, the tensor power spectrum is given by

$$\begin{aligned} \Delta_t^2(k) \simeq & \frac{181H_\star^2}{36e^3\pi^2} \left\{ 1 + \left(\log(9) - \frac{496}{181} \right) \epsilon_\star \right. \\ & + \left(\frac{\pi^2}{6} - \frac{7721}{1629} + \log(9) \right) \epsilon_\star^2 \\ & \left. + \left(\frac{\pi^2}{6} - \frac{9272}{1629} - 2 \log^2(3) + \frac{992 \log(3)}{181} \right) \epsilon_\star \delta_{\star 1} \right\} \end{aligned} \quad (54)$$

4.3 Applications to General Relativity (Cont.)

- Comparing it with the one obtained by the Green Function Method:

TABLE III: Compare the uniform approximation and Green function method

Methods	Amplitude	ϵ	ϵ^2	$\delta_1 \epsilon$
Uniform Approximation	$\frac{181H^2}{36e^3\pi^2}$	-0.543107	-0.897559	-0.439676
Green function method	$\frac{H^2}{4\pi^2}$	-0.540726	-0.967524	-0.504813
Relative difference	$\sim 0.13\%$	0.4%	7%	13%

4.3 Applications to General Relativity (Cont.)

- To the second-order approximations, the tensor power spectral index is given by

$$\begin{aligned}n_t \simeq & -2\epsilon_* + \left(\log(81) - \frac{68}{9}\right) \epsilon_*^2 + \left(\log(81) - \frac{50}{9}\right) \epsilon_* \delta_{*1} + \left(\frac{2\pi^2}{3} - \frac{3268}{81} - 8\log^2(3) + \frac{308\log(3)}{9} - \frac{4\log(64)}{81}\right) \epsilon_*^3 \\ & + \left(\frac{7\pi^2}{6} - \frac{4405}{81} - 14\log^2(3) + \frac{458\log(3)}{9} - \frac{14\log(2)}{27}\right) \epsilon_* \delta_{*1} + \left(\frac{\pi^2}{6} - \frac{433}{81} - 2\log^2(3) + \frac{50\log(3)}{9} - \frac{2\log(2)}{27}\right) \delta_* \delta_{*1}^2 \\ & + \left(\frac{\pi^2}{6} - \frac{433}{81} - 2\log^2(3) + \frac{50\log(3)}{9} - \frac{2\log(2)}{27}\right) \epsilon_* \delta_{*2}.\end{aligned}\tag{5.16}$$

4.3 Applications to General Relativity (Cont.)

- Comparing it with the one obtained by the Green Function Method:

TABLE IV: Compare the uniform approximation and Green function method

Methods	ϵ	ϵ^2	$\delta_1\epsilon$
Uniform Approximation	-2	-3.16111	-1.16111
Green function method	-2	-3.08145	-1.08145
Relative difference	0%	2.5%	7%

Table of Contents

- 1 Inflation and Planckian Physics
- 2 The Uniform Asymptotic Approximations
- 3 Power Spectra and Spectral Indices
- 4 High-order Corrections
- 5 Conclusions and Future Plan**

Conclusions and future plan

- Quantum gravitational effects in the early universe are important and need to be taken into account with the arrival of the era of precision cosmology.
- The uniform approximation method is designed to study analytically the evolution of the mode functions of perturbations generated in the early universe with such effects.
- The analytical results of power spectra and spectral indices are explicitly obtained in general case to the first-order approximations with the error bounds $\lesssim 15\%$.

Conclusions and future plan (Cont.)

- To the first-order approximations, the spectral indices are the same as those given in GR, even after these quantum effects are taken into account. But, these quantum effects indeed affect the power spectra.
- To the third-order, the analytical results of power spectra and spectral indices are explicitly obtained in the case with only one-turning point with the error bounds $\lesssim 0.15\%$.
- Applying them to GR ($\omega_k^2 = k^2$), the resulted power spectra and spectral indices are compared with the ones obtained by Green function method, and found that the relative errors are $\lesssim 0.2\%$.

Conclusions and future plan (Cont.)

- It would be very important to generalize our above studies to the cases with more than one turning point.
- Applying our method to study quantum effects from some specific models, including the ones from strong/M-Theory and loop quantum cosmology.
- Find observational signals for future experiments/ observations.
-

Acknowledgements

Work is supported in part by:

a) DOE Grant:
DE-FG02-10ER41692



b) NSFC Grant:
No. 11375153



c) Ciência Sem Fronteiras:
No. 004/2013 - DRI/CAPES



Thank You!